Determining the best practice – Optimal designs of composite helical structures using Genetic Algorithms

Jiang-Bo Bai [a], Tian-Wei Liu [a], Zhen-Zhou Wang [b],*, Qiu-Hong Lin [c], Qiang Cong [c], Yu-Feng Wang [d], Jiang-Nan Ran [d], Dong Li [a], Guang-Yu Bu [a]

[a] School of Transportation Science and Engineering, Beihang University, Beijing 100191, People's Republic of China
[b] Maritime Engineering Group, University of Southampton, Southampton, UK
[c] Beijing Institute of Spacecraft System Engineering, Beijing 100094, People's Republic of China
[d] Tianjin Institute of Aerospace Electromechanical Equipment, Tianjin 300458, People's Republic of China

ARTICLE INFO

ABSTRACT

Composite helical structures (CHSs) can store and release strain energy through elastic deformation, which have been used in automobile and aerospace structures. The compressive stiffness to weight ratio is the core in the design of these structures, requiring an optimal geometric configuration. Seven state-of-the-art Genetic Algorithms were employed and benchmarked to optimise two conflicting objectives, maximising the compressive stiffness while minimising the weight. All design variables that having effects on the compressive stiffness and weight of CHSs had been considered, which are the helix angle, the number of active coils, the helix diameter, the outer and inner diameter of cross-section, and the ply angle. A quantitative analysis method, mimicked inverted generational distance (mIGD), was used to determine the best practice of Genetic Algorithms. This study shows the selection of the Genetic Algorithm is crucial and multi-objective evolutionary algorithm based on decomposition (MOEA/D) is the best solver on searching the designs of the maximum compressive stiffness and the minimum weight.

1. Introduction

Helical structures can store strain energy to a specified displacement when load is applied, and they are widely employed at all scales in engineering. For example, the helical structures have been used as a deployable antenna to receive and transmit signals in the aerospace field [1–3] and they also have been used as a shock-absorbing spring in the automobile field to provide a comfortable ride to passengers [4,5]. Although the traditional helical structures have been widely utilised, their further development is approaching the ceiling due to their high weight, high noise and short service life. Since fibre reinforced composites have better ability of storing and releasing elastic strain energy, higher strength and lighter weight than metallic materials, they are adopted to replace the traditional helical structures. The topology of a composite helical structure (CHS) is shown in Fig. 1a. The six geometric parameters (i.e. the helix angle, the number of active coils, the helix diameter, the outer diameter and the inner diameter of cross-section, and the ply angle) significantly affect the com-

pressive stiffness and the weight of CHSs, which have been demonstrated by Liu et al. [1].

Genetic Algorithms (GAs) become the most popular tools for finding optimal composite designs in composite optimisation literature in the last 30 years [6–10]. In 1997, Yokota et al. [11] first utilised a single objective Genetic Algorithm to solve the non-linear integer programming problem of minimising the weight of metallic helical structures. Taktak et al. [12] developed a dynamic optimisation method by using a single objective Genetic Algorithm to respectively optimise the weight and the natural frequency of helical structures. Zhan et al. [13] achieved the optimal design of a CHS by using a single objective Genetic Algorithm and a response surface model. Compared with the metallic helical structure, the weight of the CHS was reduced by 34.4%. Although these studies obtained optimal designs through their single objective optimisation studies, their design solutions are not guaranteed to simultaneously satisfy other requirements. In addition, the relationship between the domain and the codomains are not discussed in these articles. The current composite literature has shown an increasing number of studies on multi-objective

---

Nomenclature

d_0	inner diameter of cross-section, mm
d_1	outer diameter of cross-section, mm
$d(\nu, O)$	the minimum Euclidean distance between ν and the points in O
D_1	helix diameter, mm
E_x	elastic modulus of composite in tangential direction, GPa
G_{xy}	shear modulus of composite in the *x-y* direction, GPa
K	compressive stiffness of CHSs, N/m
m	number of iterative calculations until CHSs fail
M^*	a set of points along the mimicked Pareto front
n	number of iterative calculations until the maximum compressive displacement of CHSs is reached without failure
N_1	number of active coils
O	a set of points from the currently obtained Pareto front
P_m	compressive failure load of the CHS, N
P_k	accumulative compressive load of the CHS, N
P_n	compressive load corresponding to the maximum displacement of the CHS, N
$\bar{P}$	mean compressive load of the CHS in the direction of helix axis, N
w	weight of CHSs, g

α_1	helix angle, deg
θ	ply angle, deg
ρ	density of composite, g/cm^3
δ_k	accumulative height variation of the CHS, mm
δ	mean compressive deformation of the CHS in the direction of helix axis, mm
$\delta_{\max}$	the maximum compressive displacement of the CHS, mm
ν	one of the points in the set M^*
CHS	composite helical structure
CNLPP	constrained non-linear programming problem
GA	Genetic Algorithm
CEC'09	IEEE congress on evolutionary computation 2009
mIGD	mimicked inverted general distance
MLSU	multilevel selection unified method
MLSGA	multi-level selection genetic algorithm
MS2L	multi-scale two-level
MOEA/D	multi-objective evolutionary algorithm based on decomposition
MTS	multiple trajectory search
NSGA-II	nondominated sorting genetic algorithm
SPEA-II	strength pareto evolutionary algorithm

optimisation of CHSs. In order to replace the traditional metallic helical structure in automobile field, Zebdi et al. [14] used a multi-objective Genetic Algorithm, nondominated sorting Genetic Algorithm (NSGA-II), to optimise a CHS and they found the best solution set (i.e. Pareto front). The results show that the population size does not influence the optimal solution, which allows designers to improve computational efficiency by reducing the population size. To obtain the maximum compressive stiffness and the minimum weight of CHSs, Ratle et al. [15] and Gobbi and Mastinu [16] both used NSGA-II to optimise the CHSs. The design solutions were verified by experimental results. However, these studies have several deficiencies. First, they have not investigated the optimal designs of CHSs that having helix angle over 10°. However, a deployable composite helical antenna often requires a large deformation space (i.e. $\alpha_1 > 10°$). Therefore, it is necessary to increase the range of the helix angle. Second, there is 'no free lunch'. If an algorithm exhibits high performance on solving a category of problems, its performance will be inevitably degraded on solving other problem types. However, the current literatures have not determined the best practice for finding the designs of the maximum compressive stiffness and the minimum weight of CHSs. NSGA-II is frequently employed to solve this problem, which is possibly due to its popularity and averagely satisfied performance on most problems as a general solver. Third, Wang and Sobey [17] pointed out that the composite optimisation works in the past ten years generally did not treat Genetic Algorithms as a specialisation. This problem is also found in the optimisation of CHSs. The best practice of Genetic Algorithms, a full spectrum of Pareto front and resolved solutions of the problem have not been investigated.

Due to the lack of studies, it is difficult to evaluate how close the currently available design solution is to the best solution. Furthermore, the best practice of Genetic Algorithms on solving this problem and the optimal designs for large deformation of CHSs, where $\alpha_1 > 10°$, remain unknown from the current composite literature. Therefore, it is necessary to determine the optimal geometric configuration of CHSs and to obtain the optimal designs of CHSs through benchmarking the state-of-the-art Genetic Algorithms. Generally, the extreme value of the objective can be obtained by solving the derivative of the analytical formula and further explore the best solution. However, for the compressive stiffness of CHSs, the analytical model proposed by Liu et al. [1] considers the geometric nonlinearity effect when determines the load-displacement relationship by accounting accumulative com-

pressive load increment and accumulative compressive deformation increment. The compressive stiffness of CHSs is obtained by using linear fitting with least square method. Therefore, gradient-based optimisation methods are not applicable. The composite literature shows that CHSs have good properties and application prospects [18–20], but there is no consensus on which design solution provides optimal performance (such as the maximum compressive stiffness and minimum weight). Montemurro and his co-authors [21–24] developed an effective multi-scale two-level (MS2L) optimisation methodology for searching the optimal designs of composite structures. The optimisation problem is split into two-scale sub-problems and formulated in the form of a constrained non-linear programming problem (CNLPP). The MS2L optimisation methodology has been utilised to solve multiple realistic engineering problems [21–24]. However, the optimisation problem in this paper is a multi-objective optimisation problem solely based on the macroscopic scale of CHSs. Therefore, the MS2L optimisation methodology was not utilised to solve the optimisation problem of this research. In this paper, seven multi-objective Genetic Algorithms were benchmarked to solve the multi-objective optimisation problem of the compressive stiffness and the weight of CHSs. Arbitrary helix angle was set in the optimisation problem to find the optimal design solutions of CHSs that satisfying the requirement of large deformation applications. The Genetic Algorithms employed for the benchmarking include: two most popular solvers, NSGA-II and strength pareto evolutionary algorithm (SPEA-II); a specialist unconstrained solver, multi-objective evolutionary algorithm based on decomposition (MOEA/D); one population based local search method, multiple trajectory search (MTS), which performs well on both unconstrained and constrained problems; and a recently developed multi-level selection genetic algorithm (MLSGA) specifically for constraint problems and the hybrid MLSGA which is suitable for problems with wide-range or discontinuous codomains, including MLSGA-NSGAII and MLSGA-MOEA/D. In the current research, each algorithm was independently run 30 cycles to eliminate the influence of the randomness of the initial population. The best practice of Genetic Algorithms was quantitatively determined by using mimicked inverted general distance (mIGD).

The paper is organised as follows: the mathematical formulations for the compressive stiffness and the weight of CHSs are detailed in Section 2; the optimisation problem formulation and the seven state-of-the-art Genetic Algorithms are introduced in Section 3; the
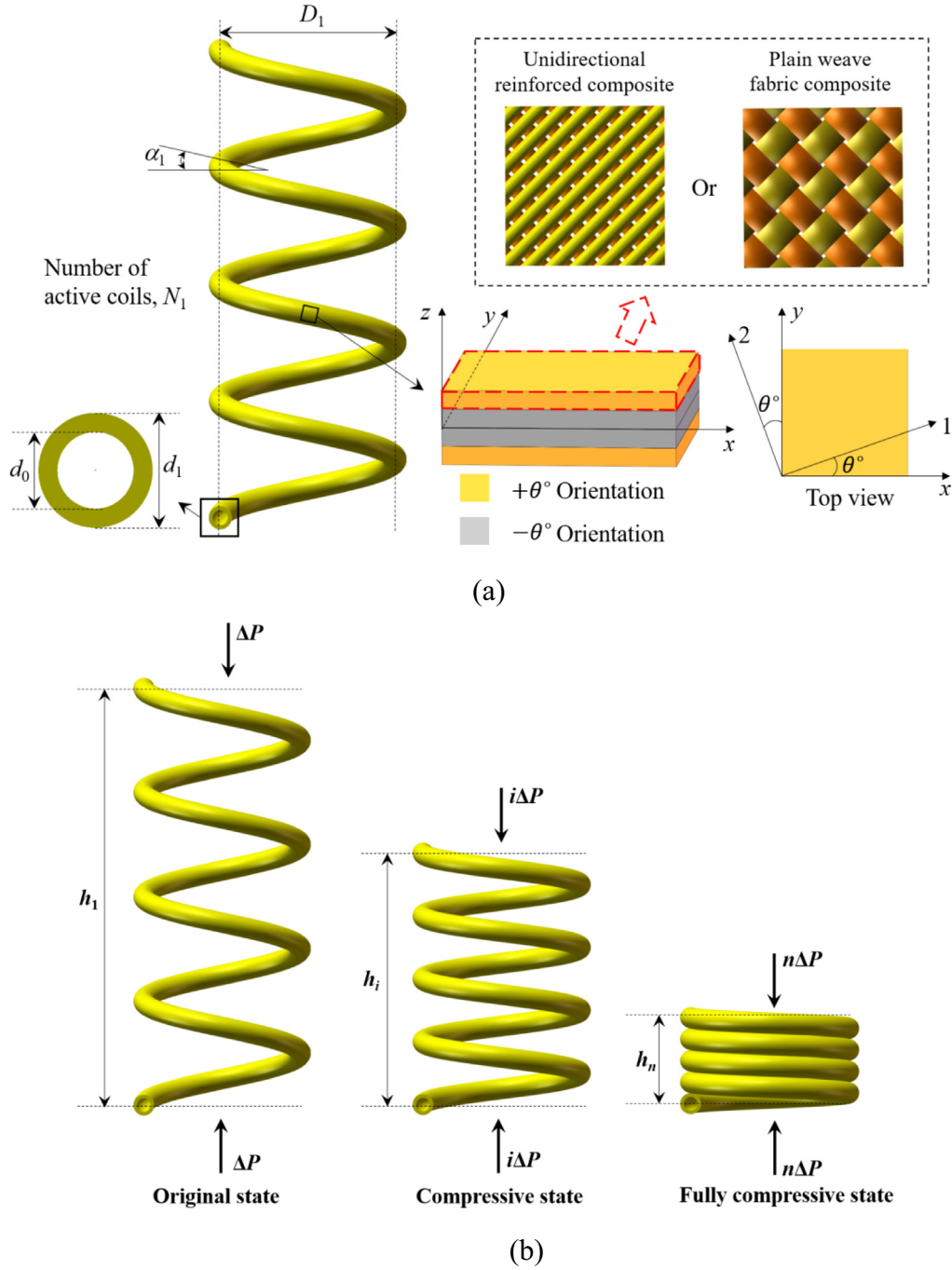
(a)

(b)

Fig. 1. Geometric configuration and compressive deformation process of a CHS [1].

benchmarking results of seven Genetic Algorithms are summarised in Section 4; the best practice and the relationship between the domain and the codomains are discussed in Section 5; the key findings have been concluded in Section 6.

2. Analytical solution for compressive stiffness and weight of composite helical structures

Based on the energy principle, Liu et al. [1] proposed an analytical model for predicting the compressive stiffness of CHSs considering geometric nonlinearity effect. The overall appearance of CHSs is helical shape and the cross-section of helix is hollow circular. The composite used to prepare CHSs can be unidirectional reinforced composite or two-dimensional fabric composite (shown in Fig. 1a). Frenet unit vectors (i.e. x, y, z = tangential, normal and binormal unit vectors) are used to describe the ply angles of CHSs. In the geometric model, the geometric parameters of CHSs change continuously with the increase of compressive load, shown in Fig. 1b. The load–displacement relationship considering geometric nonlinearity is deduced by accumulative compressive load increment and accumulative compressive deformation increment. The compressive stiffness of CHSs is obtained using linear fitting with least square method.

The details of the analytical model are referred to Liu et al. [1]. When the maximum compressive displacement of a CHS is reached without failure (shown in Fig. 1b), its compressive stiffness can be obtained by using Eq. (1),

$$K = \frac{\sum_{k=1}^{n}\left(\delta_k - \bar{\delta}\right)\left(P_k - \bar{P}\right)}{\sum_{k=1}^{n}\left(\delta_k - \bar{\delta}\right)^2} \text{ (Reaching } \delta_{\max}), \tag{1}$$

where $\bar{\delta}$ and $\bar{P}$ are respectively the mean compressive deformation and the mean compressive load of the CHS in the direction of helix axis, δ_k and P_k are the accumulative height variation and the accumulative compressive load of the CHS and $\delta_{\max}$ is the maximum compressive displacement of the CHS defined by Liu et al. [1], while n is the number of iterative calculations until the maximum compressive displacement of the CHS is reached without failure.

Liu et al. [1] compared the prediction results with the compressive stiffness of a CHS prepared by M40/epoxy648 [25] and a CHS prepared by E-glass/epoxy [16]. The relative deviations are respectively 11.35% and 0.79%, indicating that the analytical model provides an adequate accuracy for the prediction of compressive stiffness of CHSs.

The weight of a CHS is expressed in Eq. (2) as,

$$w = \frac{\pi^2\left(d_1^2 - d_0^2\right)N_1\rho D_1}{4\cos\alpha_1}, \tag{2}$$

where ρ is the density of composite, d_1 and d_0 are respectively the outer diameter and the inner diameter of cross-section, whilst N_1, D_1 and α_1 are respectively the number of active coils, the helix diameter and the helix angle.

When a CHS is compressed to closely contact with two adjacent circles without failure, the maximum compressive displacement, $\delta_{\max}$, can be obtained from the initial geometric configuration of the CHS [1] in Eq. (3) as,

$$\delta_{\max} = N_1\pi D_1\tan\alpha_1 - N_1 d_1. \tag{3}$$

The compressive load corresponding to the maximum displacement of a CHS is determined by using Eq. (4) as [1],

$$P_n = (N_1\pi D_1\tan\alpha_1 - N_1 d_1)\left\{\sum_{i=1}^{n}\frac{8N_i D_i^3}{\cos\alpha_i\left(d_1^4 - d_0^4\right)}\left[\frac{\frac{\cos^2\alpha_i}{G_{xy}} + \frac{\left(d_1^2 + d_0^2\right)\sin^2\alpha_i}{2E_x D_i^2}}{+\frac{2\sin^2\alpha_i}{E_x} + \frac{\left(d_1^2 + d_0^2\right)\cos^2\alpha_i}{G_{xy}D_i^2}}\right]\right\}^{-1}, \tag{4}$$

where E_x and G_{xy} are the elastic modulus of composite in the tangential direction and the shear modulus of composite in the x-y direction respectively. E_x and G_{xy} are determined by the properties of composites and the ply angle, θ. For more details about E_x and G_{xy}, the reader is addressed to [1].

According to the classical Tsai-Hill criterion, the compressive strength of a CHS is obtained as follows [1]:

$$P_m = \left\{\begin{array}{l} X^{-2}\left[C_1^2\left(\cos^4\theta - \sin^2\theta\cos^2\theta\right) + 8C_2^2\sin^2\theta\cos^2\theta + C_1 C_2\left(6\sin\theta\cos^3\theta - 2\sin^3\theta\cos\theta\right)\right] \\ + Y^{-2}\left[C_1^2\sin^4\theta + 4C_2^2\sin^2\theta\cos^2\theta - 4C_1 C_2\sin^3\theta\cos\theta\right] \\ + S^{-2}\left[C_1^2\sin^2\theta\cos^2\theta + C_2^2\left(\sin^4\theta + \cos^4\theta - 2\sin^2\theta\cos^2\theta\right)\right] \end{array}\right\}^{-0.5}, \tag{5}$$

where X is the longitudinal tensile or compressive strength of composite, Y is the transverse tensile or compressive strength of composite, S is the in-plane shear strength of composite, m is the number of iterative calculations until the CHS fail, while $C_1(\alpha_1, D_1, d_1, d_0, \theta)$ and $C_2(\alpha_1, D_1, d_1, d_0, \theta)$ are the transformation variables.

The reader is addressed to previous work [1] for a detailed explanation of K, $\delta_{\max}$, P_n and P_m.

3. Methodology

Wang et al. [17,26] stated that the benchmarking process is necessary when the shape of the codomains and its relationship with the domain is unknown. For the optimisation of CHSs, the benchmarking process helps understand the problem and gives the best practice of Genetic Algorithms. The multi-objective problem formulated in this paper is a non-linear constrained optimisation problem in terms of
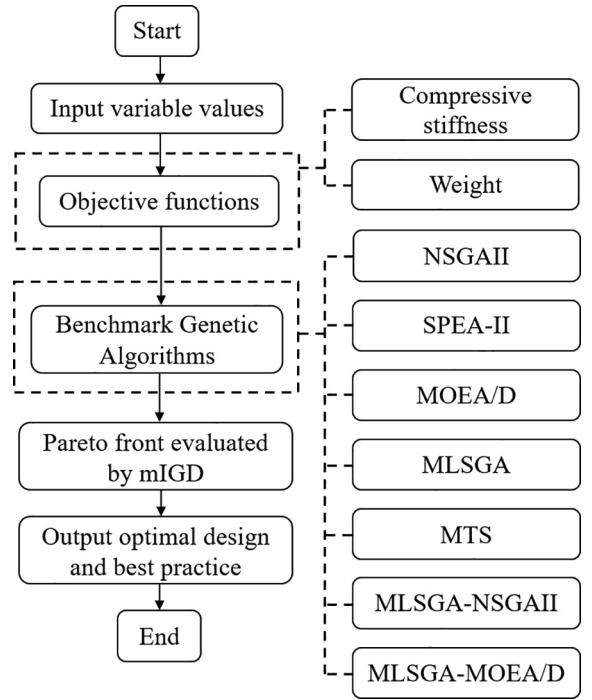

Fig. 2. General benchmarking procedure.

geometrical variables. Its non-linearity is due to the nature of the objective functions as shown in Eqs. (1) and (2), which are obtained through iterative calculations. In addition, the complexity of the problem is further improved by the geometrical constraint (i.e. the helix angle, the number of active coils, the helix diameter, the outer diameter of cross-section) shown in Eq. (3) and the mechanical constraint (i.e. the compressive strength is not reached) shown in Eqs. (4) and (5). Therefore, it is difficult to precisely select specific solvers according to the nature of the objective functions. In this case, the benchmarking results from IEEE congress on evolutionary computation 2009 (CEC'09) [27] were used to select the algorithms for the optimisation of the compressive stiffness and the weight of CHSs. NSGA-II and SPEA-II have generally good performance across all problem sets, MOEA/D performs the best on solving unconstrained problems, and one population based local search method, MTS, which comes the second and third on solving unconstrained and constrained problems. In addition, a recently developed Genetic Algorithm, MLSGA, was also included since it performs well on solving constrained problems. Hybrid MLSGAs which are suitable for wide-range or discontinuous codomains problems were employed in this study, including MLSGA-NSGAII and MLSGA-MOEA/D. A general diagram of the benchmarking process is shown in Fig. 2. All individuals from the population were evaluated through the analytical model of the compressive stiffness and the weight of CHSs.

3.1. Formulation of multi-objective optimisation problem

For a confirmed type of CHSs, the analytical model proposed by Liu et al. [1] only requires six geometric parameters to determine their compressive stiffnesses and weights. Therefore, a multi-objective optimisation problem was formulated with the six design variables. Two constraints were set, including CHSs can be compressed to the maximum compressive displacement and the compressive strength is not reached.

Concerning the geometrical design variables, they are (Fig. 1):

- the helix angle, α_1;
- the number of active coils, N_1;

- the helix diameter, D_1;
- the outer diameter of cross-section, d_1;
- the inner diameter of cross-section, d_0;
- the ply angle, θ.

The multi-objective optimisation problem of CHSs was formulated in a constrained format in Eq. (6) as,

$$\min[J(\alpha_1, N_1, D_1, d_1, d_0, \theta) = 1/K(\alpha_1, N_1, D_1, d_1, d_0, \theta), w(\alpha_1, N_1, D_1, d_1, d_0, \theta)],$$
$$subject\,to:$$
$$\begin{cases} h(\alpha_1, N_1, D_1, d_1) = \delta_{\max}(\alpha_1, N_1, D_1, d_1) - (N_1\pi D_1 \tan\alpha_1 - N_1 d_1) = 0, \\ g(\alpha_1, N_1, D_1, d_1, d_0, \theta) = 1 - \frac{P_m(\alpha_1, D_1, d_1, d_0, \theta)}{P_n(\alpha_1, N_1, D_1, d_1, d_0, \theta)} \leqslant 0, \end{cases} \quad (6)$$

where $h(\alpha_1, N_1, D_1, d_1)$ is the constraint that CHSs can be compressed to the maximum compressive displacement, $g(\alpha_1, N_1, D_1, d_1, d_0, \theta)$ is the constraint that the compressive strength is not reached, while $J(\alpha_1, N_1, D_1, d_1, d_0, \theta)$ is the inverse function of $K(\alpha_1, N_1, D_1, d_1, d_0, \theta)$.

The design space and the type of each design variable of the optimisation problem are summarised in Table 1. The analytical model can effectively predict the compressive stiffness of CHSs with arbitrary helix angle. Therefore, the range of helix angle was set between 10° and 45°, which covers the design range of the deployable composite helical antenna (i.e. large helix angle) in the aerospace field. In order to find the optimal ply angle, the range of ply angle was set between 0° and 90°. The range of each variable was determined to ensure covering all the existing applications of CHSs. The helix angle, the number of active coils, the helix diameter, the outer diameter and the inner diameter of cross-section and the ply angle are the parameters that affect the compressive stiffness, $K(\alpha_1, N_1, D_1, d_1, d_0, \theta)$, of Eq. (1), and the helix angle, the number of active coils, the helix diameter, the outer diameter and the inner diameter of cross-section are the parameters that affect the weight, $w(\alpha_1, N_1, D_1, d_1, d_0)$, of Eq. (2). In order to achieve a comprehensive Pareto front and test the performance of each benchmarked Genetic Algorithm, all design variables were set as continuous variables.

In Eq. (3) the maximum compressive displacement of CHSs, $\delta_{\max}(\alpha_1, N_1, D_1, d_1)$, is kept constant. The helix angle, the number of active coils, the helix diameter, the outer diameter of cross-section are the parameters that determine the maximum compressive displacement of CHSs in Eq. (3). The helix angle, the number of active coils, the helix diameter, the outer diameter and the inner diameter of cross-section and the ply angle are the parameters that affect the compressive load corresponding to the maximum displacement of CHSs, $P_n(\alpha_1, N_1, D_1, d_1, d_0, \theta)$, in Eq. (4). Furthermore, the helix angle, the helix diameter, the outer diameter and the inner diameter of cross-section and the ply angle are the parameters that influence the compressive failure load of CHSs, $P_m(\alpha_1, D_1, d_1, d_0, \theta)$, in Eq. (5). When P_m is higher than P_n, the CHS reaches its maximum compressive displacement while maintaining its intact condition.

Penalty techniques are general methods to deal with optimisation constraints. However, penalty techniques usually require user-defined problem-dependent parameters, which have an impact on the performance of the algorithms. Therefore, adaptive penalty techniques [28–31] have gradually become popular. Adaptive penalty techniques automatically set the values of all involved parameters using the feedback from the search process without user intervention. The penalisation coefficients are updated at each iteration on the basis of the information restrained in the genotype of the whole population. This paper utilised an adaptive penalty technique to deal with the constraints of the optimisation problem. A penalty coefficient was set in the fitness function. For any feasible solution, the penalisation coefficient was 1; for any infeasible solution, the penalisation coefficient was greater than 1. Furthermore, the penalisation coefficient was increased with the increased magnitude of the constraint violation. For more details about this method, the reader is addressed to [30].

3.2. State-of-the-art Genetic Algorithms

Due to the high nonlinearity and vary number of design variables involved into the optimisation problem, gradient-based solvers cannot be directly utilised to obtain the optimal designs of CHSs. Therefore, seven state-of-the-art Genetic Algorithms, as numerical tools, were investigated and compared for searching optimal solutions of the problem (6). Wang et al. [17,26] introduced the detailed mechanisms and parameters of NSGA-II, MOEA/D, MTS, MLSGA, MLSGA-NSGAII and MLSGA-MOEA/D. This paper also used another popular Genetic Algorithm, SPEA-II, to optimise the CHSs. SPEA-II is a widely used evolutionary algorithm and it was proposed by Zitzler et al. [32] in 2001. SPEA-II uses an external archive to hold previously found non-dominated solutions and these solutions are updated after each generation. Each individual in the archive is assigned a strength value, which also represents its fitness. An improved fitness assignment scheme is used in SPEA-II, which counts the number of solutions each individual dominates and the number of solutions dominates the individual. In order to allow a more precise guidance of the search process, a k-th nearest neighbour density estimation technique is incorporated. In addition, a new archive truncation method uses the k-th nearest neighbour density estimation technique to maintain the diversity. However, the SPEA-II algorithm generally shows the disadvantage of low computational efficiency. A detailed introduction of SPEA-II is referred to Zitzler et al. [32]. The hyperparameters of seven state-of-the-art Genetic Algorithms used within this optimisation study are listed in Table 2, where the selection, crossover and mutation types are default settings. In order to perform a fair test across the seven Genetic Algorithms the same genetic operator types: selection, crossover and mutation, used the same operator rate, which is the same as those selected for the CEC'09 benchmarking [27]. Although MTS is a population-based optimisation algorithm, it does not have crossover and mutation mechanisms. Thus, it used the same hyperparameters as those in the CEC'09 competition, except the population size and total number of function calls which are consistent with the other six algorithms.

4. Optimisation of composite helical structures

The properties of the E-glass/epoxy composite are shown in Table 3. In this paper, the material attributions of plain weave fabric composites from Gobbi and Mastinu [16] were selected since Xiong et al. [25] did not provide the strength parameters of their CHS. In addition, the CHS in Gobbi and Mastinu [16] can be compressed to the maximum compressive displacement.

4.1. Benchmarking for Genetic Algorithms

In order to obtain the maximum compressive stiffness and the minimum weight of CHSs, the influences of population size were investigated among the seven algorithms. According to the review from Wang and Sobey [17], the most frequently used number of population size is 50 and the most frequently used generation numbers are jointly 50 and 100, meaning that the most frequently used number of total

Table 1
Design space of the optimisation problem.

Design variable	Type	Lower bound	Upper Bound
α_1 (deg)	continuous	10	45
N_1	continuous	6	10
D_1 (mm)	continuous	100	150
d_1 (mm)	continuous	9.5	11.5
d_0 (mm)	continuous	7.5	8.5
θ (deg)	continuous	0	90

Table 2
Parameter definition for seven state-of-the-art Genetic Algorithms.

Algorithms	NSGA-II	MOEA/D	SPEA-II	MTS	MLSGA	MLSGA-MOEAD	MLSGA-NSGAII
No. of populations	200/to 3000	200/to 3000	200/to 3000	200/to 3000	200/to 3000	200/to 3000	200/to 3000
No. of generations	100	–	100	–	100	100	100
Stop criterion	Reach the max. generation (100)	Reach the total number of fitness evaluation	Reach the max. generation (100)	Reach the total number of fitness evaluation	Reach the max. generation (100)	Reach the max. generation (100)	Reach the max. generation (100)
Crossover rate	0.7	1	0.7	–	0.7	1	0.7
Mutation rate	0.08	0.08	0.08	–	0.08	0.08	0.08
Selector operator	NSGA-crowding distance	MOEA/D	Environmental and mating selection	–	MLSU	MOEA/D	NSGA-crowding distance
Elitism operator	Active	Active	Active	Active	Active	Active	Active

Table 3
Properties of the E-glass/epoxy composite [1].

Property	value
E_1 (GPa)	28.00
E_2 (GPa)	28.00
G_{12} (GPa)	9.50
ν_{12}	0.28
X (MPa)	473
Y (MPa)	473
S (MPa)	85
ρ(g/cm^3)	2.00

$$mIGD(O, M^*) = \frac{\sum_{\nu \in M} d(\nu, O)}{|M^*|}, \tag{7}$$

where M^* represents a set of points along the mimicked Pareto front, O represents a set of points from the currently obtained Pareto front, ν is one of the points in the set M^* and $d(\nu, O)$ calculates the minimum Euclidean distance between ν and the points in O. Lower mIGD values reflect a better quality and diversity of the Pareto front.

The mIGD values of the optimisation results obtained by each of the seven solvers were recorded from 50 generations to 300 generations with five 50-generation intervals, which are shown in Fig. 4. It is explicit that four of the seven solvers converge before reaching 300 generations, which are respectively MOEA/D, MLASG-NSGAII, NSGA-II and MTS. In contrast to the MTS and NSGA-II, the converge speed of MOEA/D and MLSGA-NSGAII are five times faster and they maintain lower mIGD values along the 300 generations. Therefore, MOEA/D and MLSGA-NSGAII perform better than MTS and NSGA-II on solving this problem. When compare the MOEA/D against MLSGA-NSGAII, the mIGD values of MOEA/D are lower along the 300 generations, indicating a better convergency and diversity of the obtained Preto front. Therefore, MOEA/D has the best performance among the four solvers, followed by MLSG-NSGAII. MOEA/D is considered having higher probability of finding resolved Pareto front. Since all mIGD values of NSGA-II, including the mean mIGD value among the 30 runs and the mIGD values from the best and worst cases, are lower than those from MTS after 100-generation and both solvers converge at 250 generations, NSGA-II is ranked in the third place and MTS is the fourth place.

It is found that this optimisation problem cannot be solved by all the seven solvers, where three solvers have not achieved converged solutions after 300 generations, which are respectively MLSGA-MOEA/D, MLSGA and SPEA-II. The mIGD values of MLSGA and MLSGA-MOEA/D gradually decrease with the increased generation number and all mIGD values of MLSGA-MOEA/D are lower than that of MLSGA. Therefore, MLSGA-MOEA/D performs better than MLSGA. It is explicit that the mIGD values from SPEA-II always maintain a high level with the increase of generation number. Therefore, it is considered that SPEA-II has the worst performance among the three algorithms.

function evaluations is 5000. In order to determine the optimal population size for each algorithm, population sizes of 200, 600, 1000, 1500, 2000 and 3000 were compared for the seven selected algorithms. The runs generating the best Pareto front from 30 simulations are illustrated in Fig. 3 for the highest and lowest population sizes for each of the seven algorithms.

It is shown in Fig. 3 that NSGA-II, MOEA/D, MTS and MLSGA-NSGAII all find continuous Pareto front with a good spread of results, covering a similar range. It is considered that the population size has little effect on these solvers. MLSGA-MOEA/D is significantly affected by the population size. When the population size is 200, only 26 points are on the Pareto front and the number of points on the Pareto front is increased with the increase of the population size. When the population size is 3000, there are 233 points on the Pareto front. They are not evenly distributed and cover all potential solutions on the Pareto front. SPEA-II is expected to have excellent performance as a general solver but the performance shown in Fig. 3 is poor. It is shown SPEA-II has inadequate ability on finding the points on the upper left and lower right of the Pareto front. The Pareto front results of MLSGA are not continuous, even as being a specialist algorithm for constrained problems. Furthermore, the influence of population size is significant on MLSGA.

4.2. Quantitative analysis for Pareto front

In order to determine the quality of the Pareto front, a convergence study was performed on the seven Genetic Algorithms at a population size of 1500. Wang and Sobey [17] proposed a mimicked inverted generational distance (mIGD) approach inspired by the inverted generational distance [27] to evaluate the accuracy and diversity of Pareto fronts. The method combines all the Pareto front solutions from all independent run cycles of all the seven algorithms that were benchmarked. Non-domination and duplication checks were implemented on this augmented Pareto front set to filter it and create a 'real Pareto front'. The mIGD values of the obtained Pareto fronts from each algorithm to this mimicked 'real Pareto front' were calculated to evaluate the performance of each benchmarked algorithm and whether the obtained Pareto front has been resolved. The mIGD is defined in Eq. (7) as,

4.3. Design schema for composite helical structures

The results of MOEA/D with 1500 population size and 200 generations were chosen to demonstrate the implications for the optimal designs of the E-glass/epoxy CHS since MOEA/D achieves the best performance among the seven solvers. Due to the repeatability of the results across the seven solvers and their 30 independent cycles, each point on the Pareto front is assumed close to the optimal designs of the E-glass/epoxy CHS. The compressive stiffness and the weight of the E-glass/epoxy experimental sample in reference [1] are respectively 1270 N/m and 108.77 g. Two points on the continuous Pareto front were manually selected to demonstrate different types of designs, namely Point A with the compressive stiffness of 1270 N/m and Point
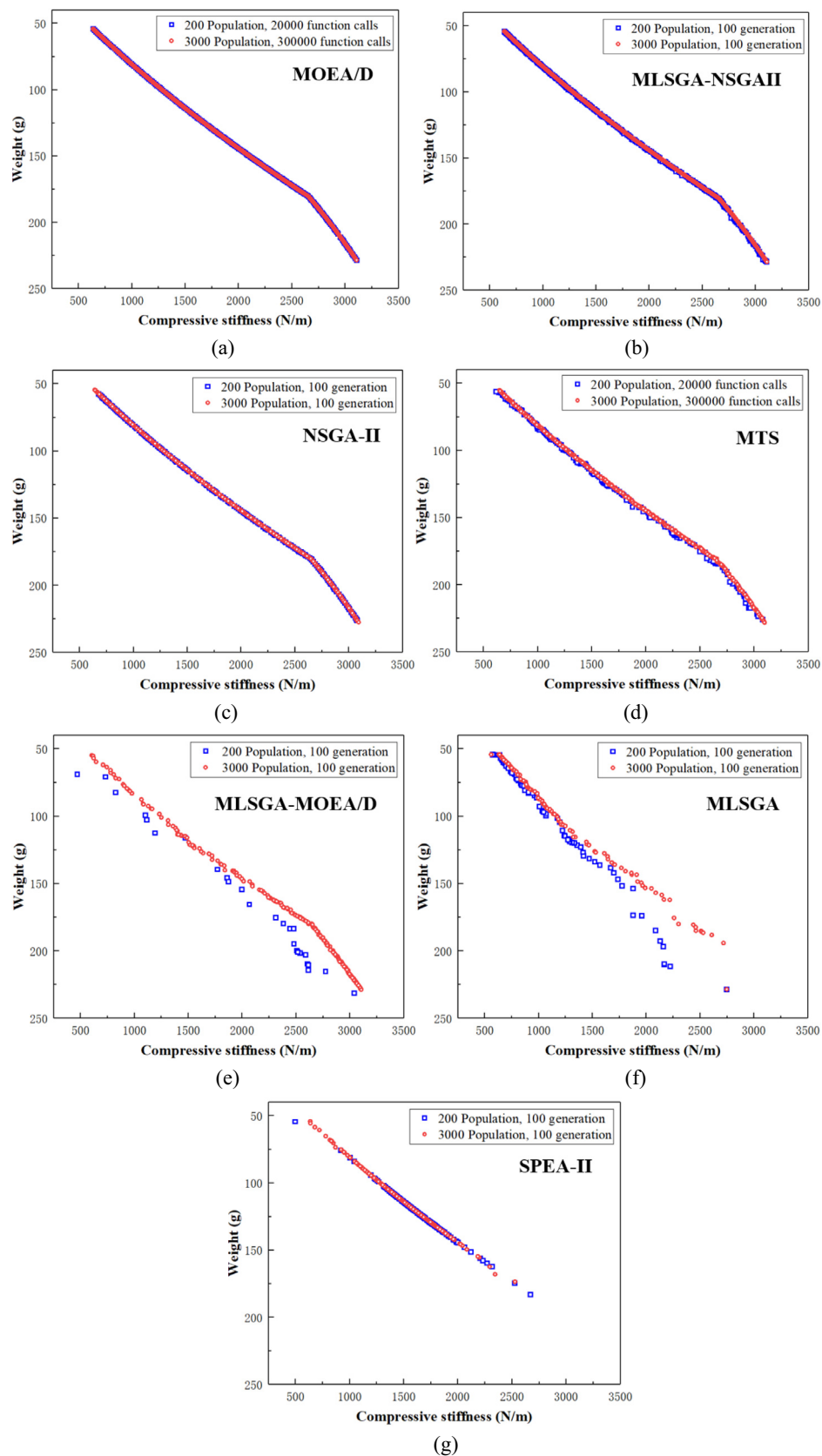
Fig. 3. Comparison of Pareto fronts for different populations sizes: (a) MOEA/D (b) MLSGA-NSGAII (c) NSGA-II (d) MTS (e) MLSGA-MOEA/D (f) MLSGA (g) SPEA-II.
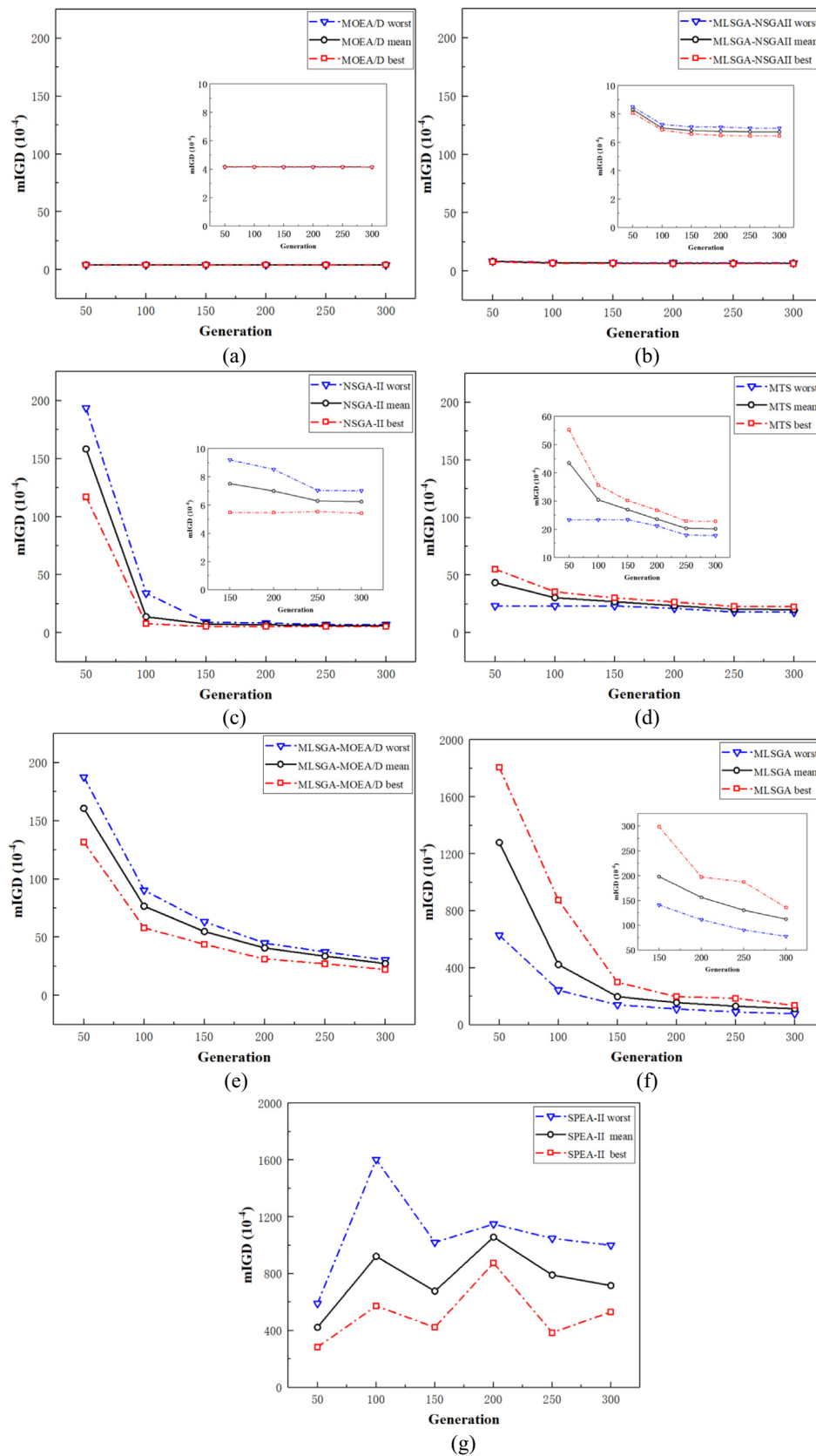
Fig. 4. Comparison of mIGD values for seven state-of-the-art Genetic Algorithms: (a) MOEA/D (b) MLSGA-NSGAII (c) NSGA-II (d) MTS (e) MLSGA-MOEA/D (f) MLSGA (g) SPEA-II.

B with the weight of 108.77 g. The location and resulting topologies of the experimental sample, Points A and B are shown in Fig. 5. There are totally 1500 examples on the entire Pareto front. Table A1 of Appendix A summarises 21 designs to demonstrate how changes in the domain affect the codomains, where the 21 designs were picked from the first point of each 75 points interval. Appendix A shows that the relationship between the objectives and the variables is nonlinear, which indicates that it is difficult to make design decisions.

For Point A, Point B and the experimental sample in Fig. 5a, the left-hand side of Fig. 5b shows the helix angle, the number of active coils, the helix diameter and the right-hand side of Fig. 5b illustrates the ply angle, the outer diameter and the inner diameter of cross-section; for the helix angle, the number of active coils and the helix diameter shown on the left-hand side, Point A, Point B and the experimental sample have the same value, which are all at the lower boundary of domain (i.e. $\alpha_1 = 10°$, $N_1 = 6$ and $D_1 = 100$ mm). For the ply angle shown on the right-hand side, although the domain of ply angle is [0°, 90°], the ply angles of Point A, Point B and the experimental sample are all close to 45°; the outer diameters and the inner diameters of Points A and B are explicitly different from those of the experimental sample. Point A and the experimental sample have the same compressive stiffness. However, when compare Point A against the experimental sample, the weight is reduced by 8.85%. Point B and the experimental sample have the same weight. However, when compare Point B to the experimental sample, the compressive stiffness is increased by 11.12%. Between these two designs, there are 65 points on the best Pareto front, providing a range of designs exhibiting different secondary properties.

In order to further analyse the relationship between the domain and the codomains, three points with special positions on the Pareto front were selected by hand, namely the left end point (Point C: $K = 635.48$ N/m and $w = 54.19$ g), the turning point (Point D: $K = 2640.75$ N/m and $w = 179.58$ g) and the right end point (Point E: $K = 3106.47$ N/m and $w = 228.50$ g), as shown in Fig. 5a. The helix angle, the number of active coils and the helix diameter of all Pareto front solutions are assigned by the minimum values of the design variable range (i.e. $\alpha_1 = 10°$, $N_1 = 6$ and $D_1 = 100$ mm), which are similar as those from Points A and B. The ply angles from Points C, D and E are oscillated around 45° (i.e. 45.36°, 44.88° and 45.89° respectively). The inner diameter of Point C is at the upper boundary of the design variable range while the outer diameter is at the lower boundary (i.e. $d_0 = 8.50$ mm and $d_1 = 9.50$ mm). Among all Pareto front solutions, Point C has the lowest compressive stiffness and the lowest weight, which are potentially applicable for ultralight and deployable composite helical antenna; the outer diameter and the inner diameter of Point D are at the maximum values of the design variable range (i.e. $d_0 = 8.50$ mm and $d_1 = 11.50$ mm); the inner diameter of Point E is the minimum value of the design variable range while the outer diameter is the maximum value of the design variable range (i.e. $d_0 = 7.50$ mm and $d_1 = 11.50$ mm), which can be used as a shock-absorbing spring due to the largest compressive stiffness.

5. Discussion

5.1. Determine the best practice through benchmarking

There is 'no free lunch', which means no algorithm can perform consistently the best on solving all types of optimisation problems. Therefore, benchmarking the state-of-the-art Genetic Algorithms on the optimisation problem of CHSs is compulsory as it may be dominated by different characteristics. Benchmarking helps to determine the dominant characteristics of the optimisation problem of CHSs and to investigate the best practice of Genetic Algorithms for this specific problem. Although general solvers such as NSGA-II and SPEA-II are expected to provide generally reasonable results, Wang et al. [17,26] pointed out that general solvers do not always perform well on solving the problems with specific characteristics.

In order to investigate the optimal designs, seven state-of-the-art Genetic Algorithms were employed to optimise the CHSs to obtain the maximum compressive stiffness and the minimum weight. The league table of the seven state-of-the-art Genetic Algorithms are summarised in Table 4. SPEA-II, as a popular general solver, cannot find the entire Pareto front, which conflicts the general expectation. It further verifies the argument of Wang et al. [17,26] that engineering optimisation problems are required to be treated specifically. Therefore, it is necessary to analyse the dominant characteristics of the optimisation problem of CHSs.

In the CEC'09 competition, MOEA/D ranks first on solving unconstrained problem and it maintains the diversity of solutions through its decomposition mechanism. MOEA/D is the best solver on solving this problem according to the results shown in Table 4. It is found that although the problem is a constrained problem, the two constraints had never been triggered from the randomly generated initial population to the Pareto front solutions during the optimisation process. MLSGA-NSGAII and NSGA-II rank second and third respectively among the seven leading algorithms. NSGA-II's mechanism is based on non-domination ranking through the whole population to find the Pareto front. The crowding distance is used to maintain the diversity of solutions in NSGA-II. In the CEC'09 competition, the hybrid MLSGAs achieve higher performance than their original algorithms. MLSGA-NSGAII utilises its own collective evolution mechanism and incorporates the crowding distance approach from the NSGA-II on the individual level to enhance the diversity of solutions. Among the seven leading Genetic Algorithms, SPEA-II has the worst performance and its performance was inadequate to find the points on the upper left and lower right of the Pareto front. However, it is found that the Pareto front has better quality and diversity with the increase of archive size. A k-th nearest neighbour density estimation technique is used in SPEA-II, where $k = \sqrt{N + \bar{N}}$. The distances of all individuals in the archive set to the k-th nearest individual are calculated and those individuals who have small distances are deleted. It guarantees the remaining individuals are evenly distributed in the optimal area. The increase of k value effectively maintains the diversity of the Pareto front. This indicates that archive size has a significant effect on the quality and diversity of the Pareto front but it is not generally considered in the composite literature. Therefore, it is considered that the dominant characteristic of this specific type of problem is the solver's ability of maintaining its solutions' diversity.

This paper focuses on the compressive stiffness and the weight of CHSs, but due to the number and diversity of points, designers are expected to find suitable geometric parameters that matching their secondary requirements, such as the shear stiffness or the natural frequency. A many-objective optimisation will dig more interesting insights for designers than the bi-objective optimisation but the complicity of the problem will be significantly increased. Insight from the current optimisation results will allow a method to be developed to include the shear stiffness and the natural frequency into the designs of CHSs.

5.2. The relationship between the domain and the codomains

In order to obtain the maximum compressive stiffness and the minimum weight of CHSs, six independent variables (i.e. the helix angle, the number of active coils, the helix diameter, the ply angle, the outer diameter and the inner diameter of cross-section) were set in this paper.

According to Fig. 5 and Appendix A, all Pareto front solutions show that the helix, the number of active coils and the helix diameter pick their minimum values in the six-dimensional domain. According to Eq. (2), when the values of these variables are smaller, the CHS is lighter; Liu et al. [1] have demonstrated that when the values of these variables are smaller, the compressive stiffness of the CHS is larger.
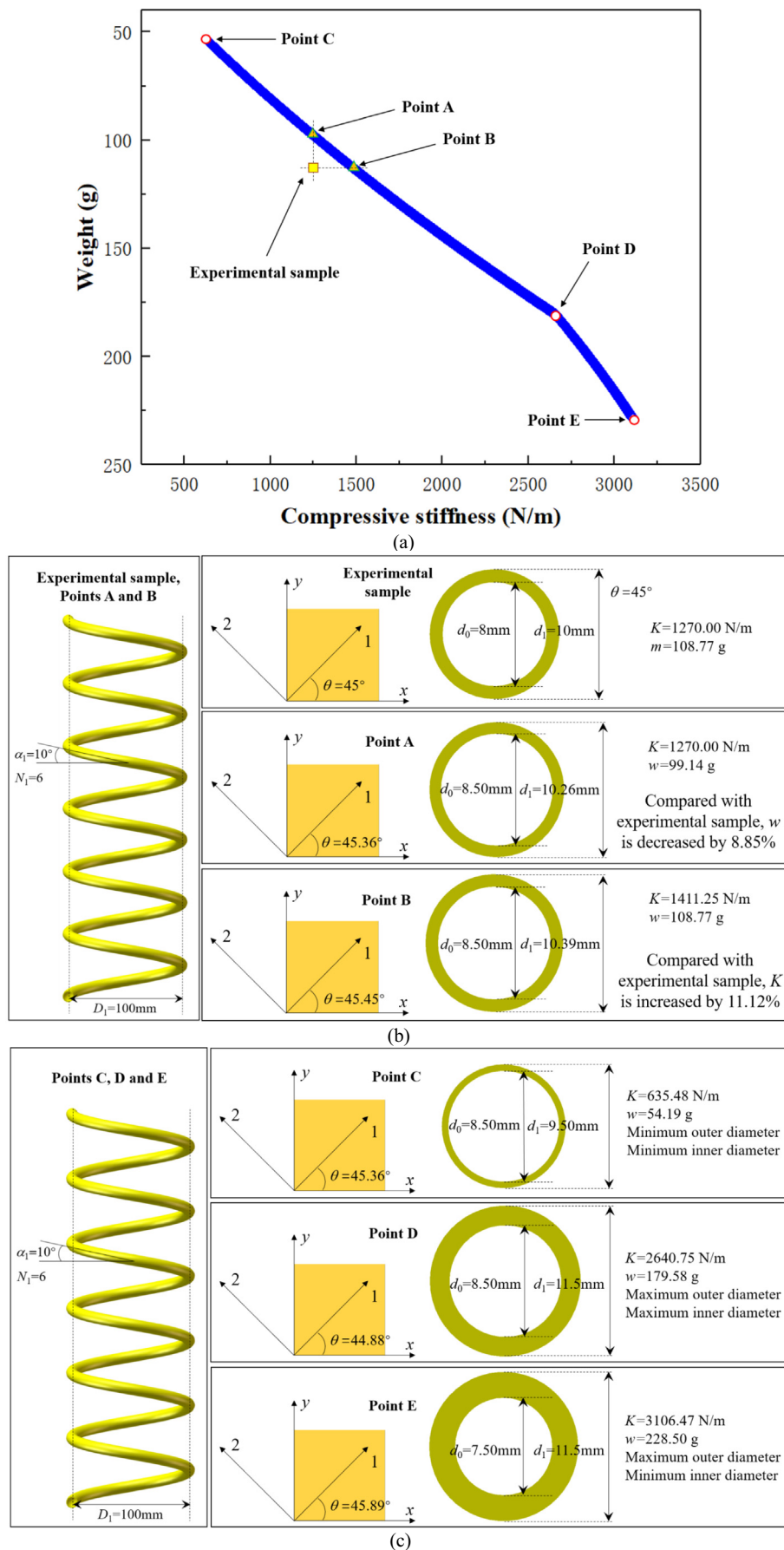
Fig. 5. Optimal designs of the E-glass/epoxy CHS: (a) sample points on Pareto front (b) the topologies of the experimental sample, Points A and B (c) the topologies of Points C, D and E.

Table 4
League table of the seven state-of-the-art Genetic Algorithms.

Genetic Algorithms	Citation frequency	Convergence	Influence of hyperparameters	Computational efficiency	Rank
MOEA/D	4761	50 Generations	Mild	High	1
MLSAG-NSGAII	9	50 Generations	Mild	Medium	2
NSGA-II	33,165	150 Generations	Medium	High	3
MTS	42	250 Generations	Medium	High	4
MLSGA	9	Non-convergence	Significant	High	5
MLSAG-MOEA/D	9	Non-convergence	Significant	High	6
SPEA-II	7165	Non-convergence	Mild	Low	7

(a)

(b)
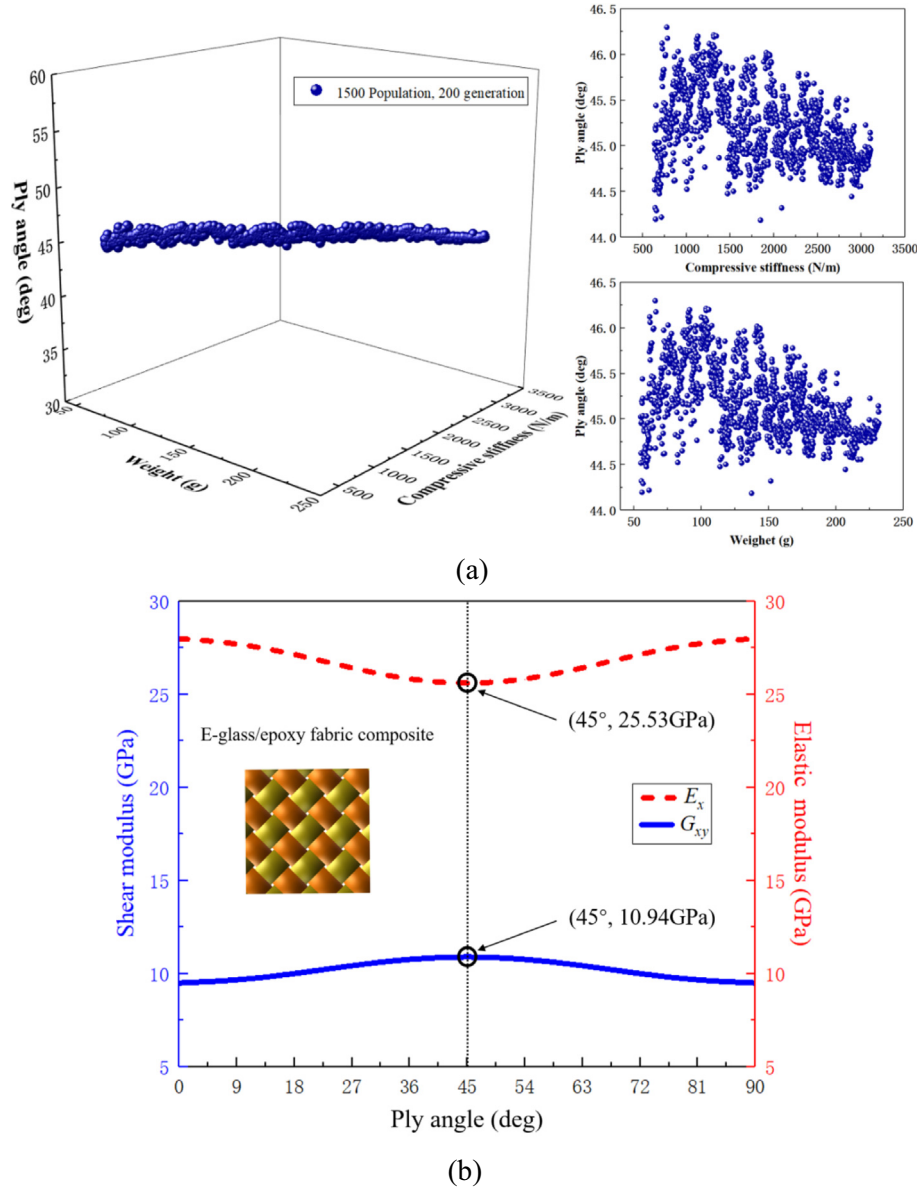
Fig. 6. The relationship between the ply angle and the codomains: (a) the ply angles of all sample points on the Pareto front (b) the effect of ply angles on E_x and G_{xy}.

Therefore, the optimisation results are consistent with the theoretical analysis.

Fig. 6a shows that the ply angles of all Pareto front solutions are oscillated within the range from 44° to 46.5°. The elastic modulus of composite in the tangential direction, E_x, and the shear modulus of composite in the x-y direction, G_{xy}, of E-glass/epoxy composite with different ply angles are illustrated in Fig. 6b. According to the constitutive model of composite [1], when the ply angle increases from 0° to

90°, E_x first decreases and then increases, reaching the minimum value at 45°; in contrast to E_x, G_{xy} increases first and then decreases, reaching the maximum value at 45°. When a CHS are subjected to external compressive load, the analytical model proposed by Liu et al. [1] points out that the smaller the helix angle of the CHS, the larger the influence of twisting moment on the strain energy. Since the helix angles of all Pareto front solutions are 10°, the twisting moment is the dominant stress, while other internal forces or moments have little influences. Liu et al.
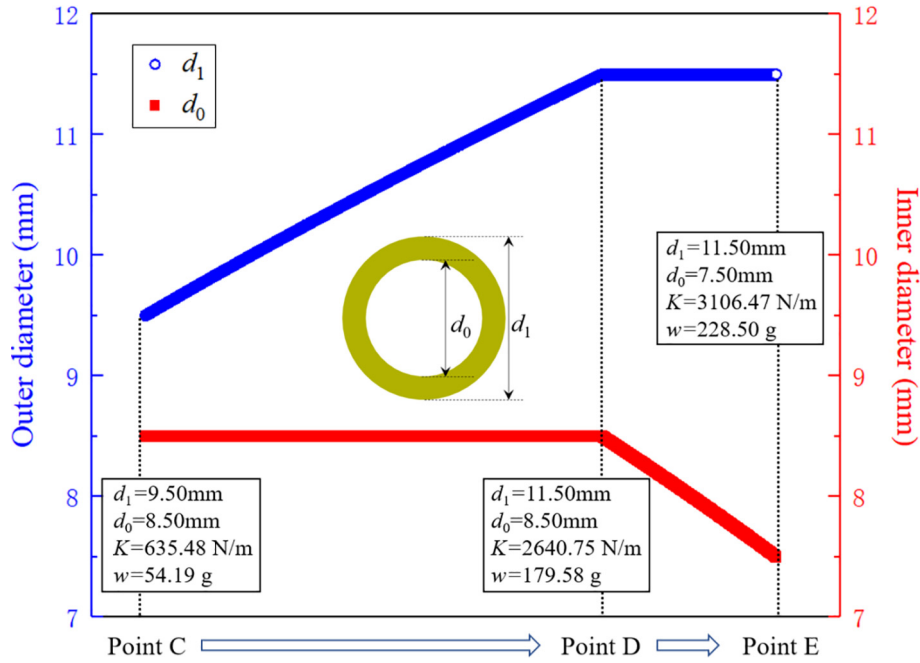
Fig. 7. The outer diameter and the inner diameter of all sample points on the Pareto front.

[1] demonstrated that when the G_{xy} is increased, the compressive stiffness of CHSs is increased. This is the main reason that the ply angles of all Pareto front solutions are between 44° and 46.5°. It is worth mentioning that the manufacturing accuracy of ply angle is difficult to reach 10^{-2} degrees, while the changes of E_x and G_{xy} are neglectable when the ply angle is between 44° and 46.5°, shown in Fig. 6b. Therefore, it is suggested to use 45° ply angle when design the E-glass/epoxy CHSs since it can significantly reduce the production cost.

However, it is difficult to determine the optimal outer and inner diameters of cross-section purely based on the theoretical model. Fig. 7 shows the outer and inner diameters of cross-section of all Pareto front solutions. According to Figs. 5 and 7, Point C at the upper left end has the smallest outer diameter and the largest inner diameter. From Points C to D on the Pareto front, the outer diameter gradually increases while the inner diameter remaining the maximum value; the turning point (i.e. Point D) has the largest outer and inner diameters. From Points D to E on the Pareto front, the inner diameter gradually decreases while the outer diameter remaining the maximum value; Point E at the lower right end has the largest outer diameter and the smallest inner diameter. The results show that the outer diameters and the inner diameters of all Pareto front solutions have at least one of the maximum or minimum values of the domain. For example, compared with the experimental sample in reference [1], Points A and B have better performance. The helix angle, the number of active coils and the helix diameter of Point A, Point B and the experimental sample have the same values (i.e. $\alpha_1 = 10°$, $N_1 = 6$ and $D_1 = 100$ mm) and similar ply angles which approximate 45°. The main differences among the three designs are the outer and inner diameters of cross-section. The inner diameters of Points A and B are at the maximum value of the domain, while the outer and inner diameters of the experimental sample are not at the boundary of the domain. In future work, the type of material may become an additional design variable. In Appendix B, the mechanical properties of a carbon/epoxy composite [14] was used to enhance the guideline on selecting the optimal designs of CHSs. The benchmarking results show that MOEA/D is still the best solver. The study shows that the rules of the helix angle, the number of active coils, the helix diameter, the outer diameter and the inner diameter of cross-section are consistent with those shown in the optimal designs of E-glass/epoxy CHSs in Section 4.3 except the ply angle. For E-glass/ epoxy CHSs, the ply angles of all Pareto front solutions are oscillated

within the range from 44° to 46.5° (Fig. 6a). However, for carbon/ epoxy CHSs, it is shown that the ply angles of all Pareto front solutions are between 11.8° and 13.5° (Fig. B3). Nevertheless, if the failure constraint is removed from the optimisation, the ply angles of all Pareto front solutions are around 45° while the rules of rest five design variables are not changed. Therefore, it is considered that for carbon/ epoxy composites the failure occurs when the ply angle is larger than 13.5°.

5.3. The guideline of efficiently selecting the optimal designs of composite helical structures

Although Genetic Algorithms can obtain the optimal designs of CHSs that simultaneously satisfying multiple requirements (i.e. the maximum compressive stiffness and the minimum weight), the optimisation process is relatively time-consuming and complex. However, using the relationship of the design domain and the codomains found from this paper, engineers can determine the optimal design variables in their applications through simple calculation rather than re-running the Genetic Algorithms. For the helix angle, the number of active coils and the helix diameter, the designer should select the minimum values of the domain; for the ply angle, the designer should select 45° since the compressive stiffness of CHSs is commonly the highest when the ply angle is about 45° for different types of composites. However, it is not guaranteed that the optimal designs with 45° ply angle always remain intact during compression, such as the carbon/epoxy CHSs shown in Section 5.2. The failure significantly depends on the longitudinal and transverse tensile or compressive strengths and the in-plane shear strength of the material. Therefore, the designer is recommended to use $g(\alpha_1, N_1, D_1, d_1, d_0, \theta)$ of Eq. (6) to check whether using 45° ply angle causes the failure of their CHSs. If the CHSs remain intact, the designer achieves the optimal designs; if the CHSs fail, it is necessary to use the MOEA/D to obtain the optimal designs of CHSs. For the outer and inner diameters of cross-section, the designer can firstly obtain the compressive stiffness and the weight of Points C, D and E on the Pareto front according to the boundaries of domain of the outer and inner diameters. If the minimum weight required by the designer is within the range corresponding to the weight of Points C and D, the maximum value of inner diameter of domain should be selected. Then the corresponding outer diameter value can be solved according to Eq.

Table A1

Samples of optimal designs for E-glass/epoxy composite.

	Compressive stiffness (N/m)	Weight (g)	d_1 (mm)	d_0 (mm)	θ (deg)
1	635.48	54.19	9.50	8.50	45.04
2	769.52	64.22	9.67	8.50	45.16
3	908.07	74.31	9.84	8.50	44.98
4	1048.83	84.21	10.01	8.50	45.69
5	1190.52	93.86	10.17	8.50	44.66
6	1332.10	103.22	10.32	8.50	45.55
7	1472.88	112.27	10.46	8.50	45.34
8	1611.94	120.98	10.61	8.50	44.85
9	1748.88	129.33	10.74	8.50	45.10
10	1882.79	137.33	10.86	8.50	45.35
11	2013.51	144.96	10.98	8.50	45.70
12	2140.63	152.23	11.09	8.50	45.62
13	2265.68	159.24	11.19	8.50	45.37
14	2384.75	165.81	11.29	8.50	45.55
15	2499.97	172.06	11.38	8.50	44.92
16	2611.04	177.99	11.47	8.50	44.91
17	2711.71	185.71	11.50	8.40	44.77
18	2807.57	195.29	11.50	8.20	45.33
19	2904.69	205.47	11.50	7.99	44.71
20	3004.03	216.45	11.50	7.76	45.04
21	3106.47	228.50	11.50	7.50	44.85

Note: The helix angles of all samples are 10°, the number of active coils are 6, and the helix diameters are 100 mm (i.e. $\alpha_1 = 10°$, $N_1 = 6$ and $D_1 = 100$ mm).

Table B1

Properties of a carbon/epoxy composite [14].

Property	value
E_1 (GPa)	111.67
E_2 (GPa)	5.83
G_{12} (GPa)	3.50
ν_{12}	0.21
X (MPa)	1058
Y (MPa)	117.5
S (MPa)	52.5
ρ(g/cm^3)	1.28

(2) and finally the compressive stiffness of CHSs can be solved using the values of all independent variables. If the designer determines the required maximum compressive stiffness, then the six design variables and the minimum weight can be determined in the same way. Using the proposed guideline, the efficiency of searching the optimal designs of CHSs will be significantly increased in the practice.

6. Conclusions

Composite helical structures (CHSs) are increasingly used in aerospace and automotive fields. It is necessary to optimise CHSs to obtain the optimal compressive stiffness and weight. In this paper, Genetic Algorithms were employed to find the optimal geometric configuration of CHSs which can be compressed to the maximum compressive displacement. Seven state-of-the-art Genetic Algorithms were benchmarked. The MOEA/D is the best solver, which was determined by a quantitative analysis method, mIGD metric. As general solvers, NSGA-II and SPEA-II were expected to provide top performance, but SPEA-II exhibited poor performance and NSGA-II did not exhibit top performance on searching the optimal designs of CHSs. The dominant characteristic of this specific type of problem is the solver's ability of maintaining its solutions' diversity. Without investigating the dominant characteristic, the selection of the Genetic Algorithms is critical to find the optimal solutions.

Among the achieved Pareto front solutions, Point A has the same weight as the experimental sample [1] but the compressive stiffness is increased by 11.12%. Point B has the same compressive stiffness as the experimental sample [1] but the weight is reduced by 8.85%.

The relationship between the six-dimensional domain and the two-dimensional codomains was analysed. A design guideline of CHSs is proposed in this paper to help the designers to efficiently determine their required designs. The guideline recommends that the helix angle, the number of active coils and the helix diameter are required to be their minimum values in the domain during the design process to achieve the maximum compressive and the minimum weight. The ply angle is ideally chosen 45°. However, the designer is recommended to use $g(\alpha_1, N_1, D_1, d_1, d_0, \theta)$ of Eq. (6) to check whether using 45° ply angle causes the failure of their CHSs. If the CHSs remain intact, the designer achieves the optimal designs; if the CHSs fail, it is necessary to use the MOEA/D to obtain the optimal designs of CHSs. Furthermore, the guideline demonstrates that the outer and inner diameters of cross-section are the main variables affecting the distribution of Pareto front solutions.

CRediT authorship contribution statement

Jiang-Bo Bai: Supervision, Resources, Project administration. **Tian-Wei Liu:** Investigation, Validation, Writing - original draft. **Zhen-Zhou Wang:** Supervision, Methodology, Writing - review & editing. **Qiu-Hong Lin:** Resources. **Qiang Cong:** Resources. **Yu-Feng Wang:** Resources. **Jiang-Nan Ran:** Resources. **Dong Li:** Investigation. **Guang-Yu Bu:** Investigation.

Declaration of Competing Interest

The authors declare that they have no known competing financial interests or personal relationships that could have appeared to influence the work reported in this paper.

Acknowledgements
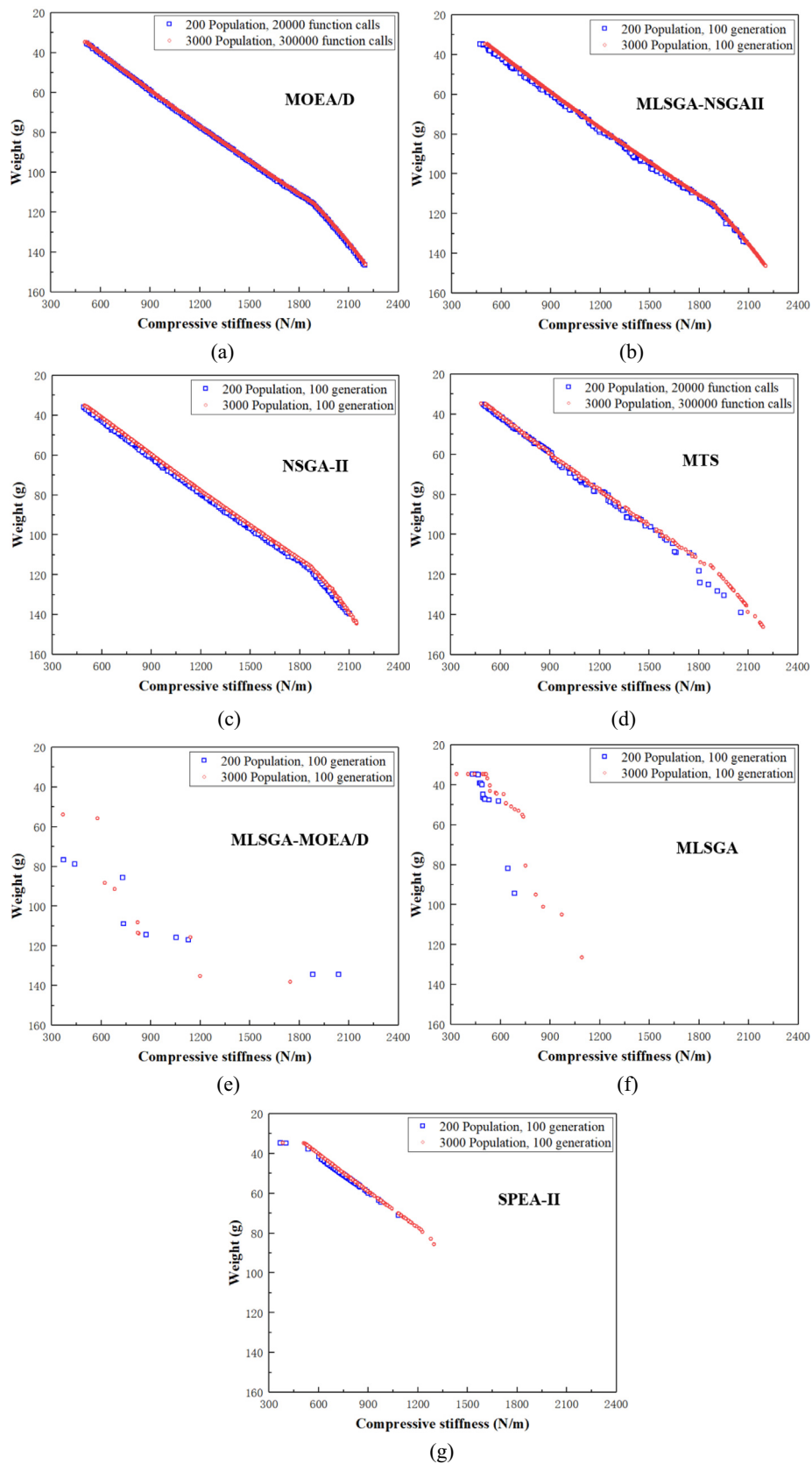
Appendix

A. Samples of optimal designs

Fig. B1. Comparison of Pareto fronts for different populations sizes: (a) MOEA/D (b) MLSGA-NSGAII (c) NSGA-II (d) MTS (e) MLSGA-MOEA/D (f) MLSGA (g) SPEA-II.
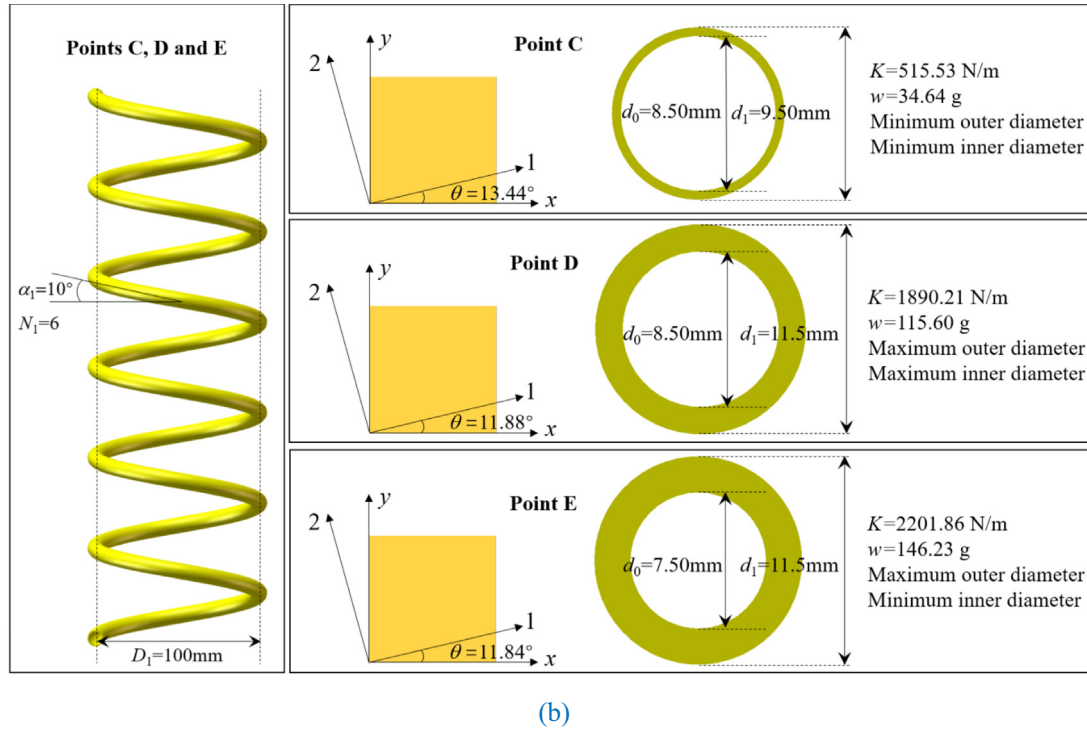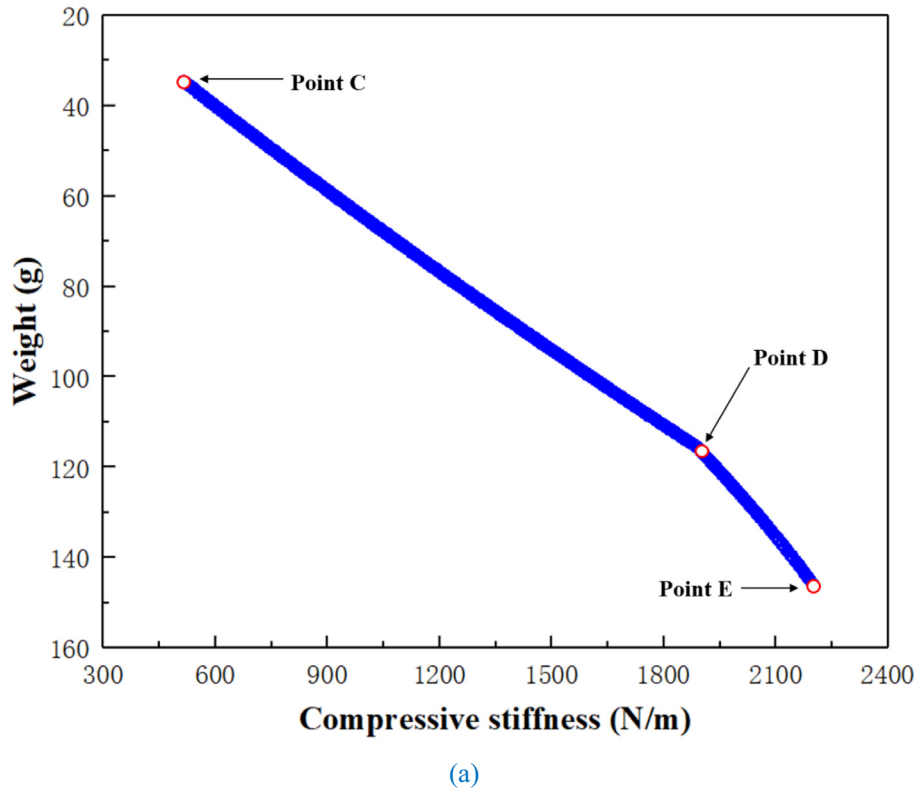
(a)

(b)

Fig. B2. Optimal designs of the carbon/epoxy CHS: (a) sample points on Pareto front (b) the topologies of Points C, D and E.

Appendix B. Optimal designs of composite helical structures using a carbon/epoxy composite

In order to enhance the guidelines on selecting the optimal designs of CHSs, another material selected from Zebdi et al. [14] was used as a validation case. Table B1 summarises the material properties of a carbon/epoxy composite. Similarly, the seven Genetic Algorithms were benchmarked to optimise the carbon/epoxy CHS and the hyper-

parameters were kept consistent with those in Section 3.2. The run generating the best Pareto front from the 30 simulations are shown in Fig. B1.It is explicit that MOEA/D, MLSGA-NSGAII and NSGA-II perform better than the rest solvers among the seven Genetic Algorithms. MOEA/D has the lowest mIGD value, indicating a better convergency and diversity of the obtained Pareto front. The mIGD value of MLSGA-NSGAII is lower than that of NSGA-II. Therefore, MOEA/D has the best performance among the three solvers, while MLSGA-NSGAII is ranked
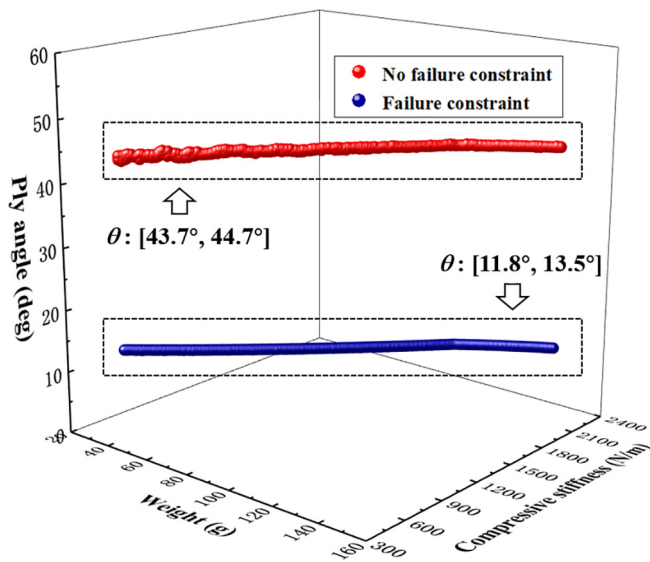
Fig. B3. The relationship between the ply angle and the codomains.

in the second place and NSGA-II is the third place. The results are consistent with those shown in Sections 4.1 and 4.2. Therefore, the Pareto front results of MOEA/D were chosen to analyse the implications for the types of materials on the optimal designs of CHSs. The locations and the resulting topologies of Points C, D and E are shown in Fig. B2. The relationship between the ply angle and the codomains are shown in Fig. B3.

References

[1] Liu TW, Bai JB, Lin QH, et al. An analytical model for predicting compressive behaviour of composite helical Structures: considering geometric nonlinearity effect. Compos Struct 2021;255:112908.
[2] Cheng Y, Chen L, Chen X. A beam scanning method based on the helical antenna for space-based AIS. J Navigation 2015;68(1):52–70.
[3] Sproewitz T, Block J, Bager A, et al. Deployment verification of large CFRP helical high-gain antenna for AIS signals. Aerospace Conference, 2011 IEEE.
[4] Gzal M, Groper M, Gendelman O. Analytical, experimental and finite element analysis of elliptical cross-section helical spring with small helix angle under static load. Int J Mech Sci 2017;130:476–86.
[5] Wu JJ. Study on the inertia effect of helical spring of the absorber on suppressing the dynamic responses of a beam subjected to a moving load. J Sound Vib 2006;297(3–5):981–99.
[6] Kudela P, Radzienski M, Fiborek P, et al. Elastic constants identification of woven fabric reinforced composites by using guided wave dispersion curves and genetic algorithm. Compos Struct 2020;249:112569.
[7] Ehsani A, Dalir H. Multi-objective optimisation of composite angle grid plates for maximum buckling load and minimum weight using genetic algorithms and neural networks. Compos Struct 2019;229:111450.
[8] Petrone G, Meruane V. Mechanical properties updating of a non-uniform natural fibre composite panel by means of a parallel genetic algorithm. Compos A Appl Sci Manuf 2017;94:226–33.
[9] Badalló P, Trias D, Marín L, et al. A comparative study of genetic algorithms for the multi-objective optimisation of composite stringers under compression loads. Compos B Eng 2013;47:130–6.
[10] Talebitooti R, Gohari HD, Zarastvand MR. Multi objective optimisation of sound transmission across laminated composite cylindrical shell lined with porous core investigating Non-dominated Sorting Genetic Algorithm. Aerosp Sci Technol 2017;69:269–80.
[11] Yokota T, Taguchi T, Gen M. A solution method for optimal weight design problem of helical spring using genetic algorithms. Comput Ind Eng 1997;33:71–6.
[12] Taktak M, Omheni K, Aloui A, et al. Dynamic optimisation design of a cylindrical helical spring. Appl Acoust 2014;77:178–83.
[13] Zhan BW, Sun LY, Huang BC, et al. Design and optimisation of automotive composite helical spring. J Beijing Univ Aeronaut Astronaut 2018;44(7):1520–7.
[14] Zebdi O, Boukhili R, Trochu F. Optimum design of a composite helical spring by Multi-criteria Optimisation. J Reinf Plast Compos 2009;28(14):1713–32.
[15] Ratle F, Lecarpentier B, Labib R, et al. Multi-objective optimisation of a composite material spring design using an evolutionary algorithm. Berlin Heidelberg: Parallel Problem Solving from Nature-PPSN VIII. Springer; 2004.
[16] Gobbi M, Mastinu G. On the optimal design of composite material tubular helical springs. Meccanica 2001;36(5):525–53.
[17] Wang ZZ, Sobey A. A comparative review between Genetic Algorithm use in composite optimisation and the state-of-the-art in evolutionary computation. Compos Struct 2020;233:111739.
[18] Ke J, Wu ZY, Liu YS, et al. Design method, performance investigation and manufacturing process of composite helical springs: a review. Compos Struct 2020;252:112747.
[19] Choi BL, Choi BH. Numerical method for optimizing design variables of carbon-fiber-reinforced epoxy composite coil springs. Compos B Eng 2015;82:42–9.
[20] Renugadevi K, Devan PK, Thomas T. Fabrication of calotropis gigantea fibre reinforced compression spring for light weight applications. Compos B: Eng 2019;172:281–9.
[21] Montemurro M, Catapano A. A general B-Spline surfaces theoretical framework for optimisation of variable angle-tow laminates. Compos Struct 2019;209:561–78.
[22] Fiordilino GA, Izzi MI, Montemurro M. A general isogeometric polar approach for the optimisation of variable stiffness composites: application to eigenvalue buckling problems. Mech Mater 2021;153:103574.
[23] Izzi MI, Montemurro M, Catapano A, et al. A multi-scale two-level optimisation strategy integrating a global/local modelling approach for composite structures. Compos Struct 2020;237:111908.
[24] Montemurro M, Izzi MI, El-Yagoubi J, et al. Least-weight composite plates with unconventional stacking sequences: design, analysis and experiments. J Compos Mater 2019;53(16):2209–27.
[25] Xiong ZY, Song RX, Kang ZX, et al. Analysis on rigidity of composite helical spring and its influence factors. Engineering Mechanics, 2015, 32(9):216-221 and 228.
[26] Wang ZZ, Bai JB, Sobey A, et al. Optimal design of triaxial weave fabric composites under tension. Compos Struct 2018;201:616–24.
[27] Zhang Q, Suganthan PN. Final report on CEC'09 MOEA competition. In: Congress on evolutionary computation (CEC 2009), 2009.
[28] Montemurro M, Vincenti A, Vannucci P. The Automatic Dynamic Penalisation method (ADP) for handling constraints with genetic algorithms. Comput Methods Appl Mech Eng 2013;256:70–87.
[29] Karafotias G, Hoogendoorn M, Eiben AE. Parameter control in evolutionary algorithms: trends and challenges. IEEE Trans Evol Comput 2015;19(2):167–87.
[30] Barbosa HJC, Lemonge ACC, Bernardino HS. A critical review of adaptive penalty techniques in evolutionary computation. Evolutionary Constrained Optimization 2015:1–27.
[31] Aleti A, Moser I. A systematic literature review of adaptive parameter control methods for evolutionary algorithms. ACM Comput Surv 2016;49(3):1–35.
[32] Zitzler E, Laumanns M, Thiele L. SPEA2: Improving the strength pareto evolutionary algorithm. 2001:95-100.